J Therm Anal Calorim (2018) 131:799–810
https://doi.org/10.1007/s10973-017-6577-9

Thermal and electrochemical studies of Cu(II) 8-hydroxyquinoline organophilic montmorillonite

Caroline Polini Lupi[1,2] · Bruno Trevizan Franzin[1,2] · Paulo Roberto Pereira[1] · Airton Juliano Damaceno[2] · Tony Rogério de Lima Dadamos[2] · Cecilia Cristina Marques dos Santos[3] · Iêda Aparecida Pastre[2] · Fernando Luis Fertonani[2]

Received: 5 August 2016 / Accepted: 13 July 2017 / Published online: 27 July 2017

Abstract The thermal and electrochemical behavior of montmorillonite clay-8-hydroxyquinoline (8-HQ) film was studied in the absence and presence of aqueous Cu(II) ions. The suggested formation of the ternary complex type: $\{Pt/[> Si–O]_n[Cu(II)(OH_2)_n(8\text{-}HQ)_k]\}^{3-n-k}$, with thermal stability up to 350 °C, was studied, based on UV-spectroscopy, thermal (DTG-DSC, molecular fluorescence and XRD. The Pt/binary composite film (SWy-1:8-HQ) interphase composed of montmorillonite (SWy-1) with 8-hydroxyquinoline (8-HQ) was investigated by electrochemical techniques analyzing the cyclic voltammograms (CVs) obtained at different scan rates (v) and copper(II) ion concentrations. The mechanical stability of the thin films was demonstrated by performing 80 successive voltammetric cycles. Two pairs of redox peaks, indicated by peaks A/D and C/B were observed. For Cu(II) ions in solution, the log $i_p \times \log v$ relationships showed processes controlled by adsorption, peaks A/D, and by diffusion, peaks C/B. The analysis of $i_p/v^{1/2}$ and i_{pa}/i_{pc} versus v suggested two homogeneous coupled reactions, being both reversible and fast kinetic chemical reactions, associated to the mechanisms chemical-electrochemical (CE) and electrochemical-chemical (EC), respectively. The modified electrode showed a good sensitivity to low concentrations of Cu(II) ions, which opens the possibility of being used in chemical analysis.

Keywords Organic montmorillonite composites · TG–DTA simultaneous, Cu(II) ions · Reversible coupled reactions · Cu(I)/Cu(II) redox species

Introduction

The metal ions are introduced into the environment in different ways, either by natural phenomena or by human activity. The presence of metal ions in the environment can lead to an accumulation in different environmental compartments, especially the contamination of drinking water supplies and the living organisms in these media that can be present in foods, even in small amounts, representing a health risk to humans, as they are not biodegradable. One of its main anthropogenic sources is the release of wastewater with an excess of metal ions as a result of widespread use in industrial processes [1].

The copper element is naturally found in an elementary form and in different compounds. The most toxic state of copper is the divalent oxidation state, Cu(II). As regards human activity, copper is used profusely in manufacturing various metallic and electrical equipment alloys being released into the environment, mainly through mining, agricultural processes, solid waste disposal, welding and electroplating, liquid effluent from sewage treatment plants, old metallic plumbing materials (pipes, taps, braces, and various forms of tubes) and electrical wiring [2].

Some metal elements are essential to human life, such as iron, zinc, copper, chromium, cobalt and manganese.

Electronic supplementary material The online version of this article (doi:10.1007/s10973-017-6577-9) contains supplementary material, which is available to authorized users.

✉ Fernando Luis Fertonani
fertonan@ibilce.unesp.br

[1] Departamento de Química Analítica, Instituto de Química/IQ/UNESP, Campus Araraquara, Araraquara, SP, Brazil

[2] Departamento de Química e Ciências Ambientais/IBILCE/Unesp, Campus São José do Rio Preto, São José do Rio Preto, SP, Brazil

[3] Instituto Adolpho Lutz - IAL, São José do Rio Preto, SP, Brazil

Although they are essential to human life, in an excessive intake may become toxic. On the other hand, lead, nickel, cadmium and mercury are toxic at low levels. The toxic elements can produce deleterious effects when taken for a long time, even at low concentrations [3].

The copper ion is an important bio-element for human life and plays a significant role as a co-factor for many important enzymes. Studies of samples of this metal ion are of great importance due to its critical biological effects as an essential element. However, at high levels it becomes toxic, causing a metal taste in the mouth, nausea, vomiting, irritation of the nasal and throat tract, stomach pain, ulcer, cerebral injury and liver damage and so on [4]. Thus, it is extremely necessary to control and remove copper ions from water samples [5] and food [6] eaten daily among other matrices.

Several analytical methods have been proposed for the determination of copper ions in different matrices such as water, food, plants, soil samples among others: pre-concentration by gas-assisted dispersive liquid phase microextraction (GA-DLPME) and spectrophotometric determination of Cu(II) ions in various samples of water [7]; FAAS used in the determination of copper ions [8], zinc, nickel and iron into gasoline by pre concentration of silica gel modified with 2-aminothiazole groups (SiAT) [9]; application of Isotope Dilution Inductively Coupled Plasma Mass Spectrometry (ID ICP-MS) for determining the total mass fractions of trace elements Cu, Cd, Hg, Pb and Zn in sea sediment [10]; chemical speciation of Cu in food by X-ray Absorption Near-Edge Structure (XANES) [11]; colorimetric detection of Cu(II) ions by optical chemo-sensor for visual detection in the water and biological samples [12]. Several techniques are also being employed, e.g., inductively coupled plasma emission spectrometry [13], neutron activation analysis [14], electrothermal atomic absorption spectrometry [15], chromatography [16], and electroanalytical techniques such as anodic [17] and cathodic [18] stripping voltammetry, differential pulse anodic stripping voltammetry [19, 20], and cyclic voltammetry [21, 22].

The electroanalytical techniques are noteworthy due to their simplicity in terms of construction and analysis, short time-analysis, low cost when compared to the others, low wastage and of solvent consumption, environmentally friendly, and its versatility and mobility with good sensitivity and selectivity. Thus, several studies using conventional and modified electrodes have been developed for determination of copper and other metal ions. Using the adsorptive voltammetry technique, a modified carbon paste electrode was employed for the determination of Cu^{2+} ions [23]. The anodic stripping with differential pulse was used with a carbon nanotube paste electrode (NTC) modified with cysteine for Cu^{2+} [24] and Pb^{2+} the determination [24, 25]. Another NTC electrode modified with fluoride was developed for determining Cu^{2+} ions by adsorptive stripping voltammetry [26].

Chemically modified electrodes (CMEs) are electrodes having their surfaces modified by an active species, which gives the original electrodes different physic-chemical characteristics such as reactivity and selectivity. These different characteristics have attracted attention in the electrochemistry and electroanalytical fields, and show a growth in these fields. Employment of modified electrodes, specifically clays, as proposed in the present study, is a field in constant development, and increasingly new methods of preparation are reported in literature for various matrices [21, 27–33]. Several studies showed the application of modified electrodes for metal ion determination in aqueous solutions, some of them employing a modification process with clays and organoclays [34–41].

Thus, the purpose of this paper is to study: (1) the behavior of the montmorillonite-8-hydroxyquinoline composite (SWy-1:8-HQ) in the presence and the absence of Cu(II) ions, by thermal (DTG–DTA and DSC), XRD, UV–visible and molecular fluorescence spectroscopic techniques, and electrochemical techniques; (2) the elucidation of the global electrochemistry mechanism of SWy-1:Cu(II)-8-HQ ternary composite. The aim is also to demonstrate: (1) the ease and speed of the preparation of electrodes (repeatability); (2) the speed of the experimental work development; (3) its mechanical and thermal stability that allows its reuse; and (4) its low cost in relation to the chemical compounds used (clay and 8-HQ) and its reuse. The characteristics of this system, [SWy-1:8-HQ], make future applications possible e.g., as quantitative electrochemical determination Cu(II) ions and also as adsorbents for wastewater and an urban water purification process, as detailed in a similar study which employed Fe(III) ions [42] in the compound of montmorillonite-8-hydroxyquinoline (SWy-1:8-HQ).

Experimental

Preparation of SWy-1 composites: [SWy-1:Cu$(OH_2)_n$]; [SWy-1:8-HQ]; [SWy-1:Cu(II):8-HQ)]; and [SWy-1:8-HQ:Cu(OH_2)]

For electrochemical and spectroscopic studies, an aqueous suspension of SWy-1 was previously prepared [42] and pure solid 8-hydroxyquinoline (8-HQ) was added in a proportion of 10% mass and maintained under mechanical stirring for 24 h; generating the binary composite, SWy-1:8-HQ. For the studies in solid state a methanolic suspension of SWy-1:8-HQ was likewise prepared for the aqueous suspension described above. In one portion of suspension of SWy-1:8-HQ, Cu(II) ions were added from a

stock solution of $Cu(SO_4).5H_2O$ with a concentration of 5.00×10^{-3} mol L^{-1} and maintained under mechanical stirring for another 24 h, generating the ternary composite, SWy-1:8-HQ-Cu(II). Then, the resulting suspensions were dried under a laboratory fume exhaust hood for 24 h, producing the solid binary and ternary composites. Thermal analysis (TG/DTG and TG–DTA), XRD were performed on these samples.

Electrode surface modification

The SWy-1:8-HQ prepared suspension, as previously described, was stirred for 12 h, and increments of 0.5 μL were applied on top of the platinum in order to cover the entire surface. The solvent was evaporated in a forced circulation air stove at 50 °C for 20 min. The procedure was repeated five times.

Electrochemical measurements with {Pt/[SWy-1:8-HQ]} thin solid film electrode

Cyclic voltammetric experiments were performed with $E_{start} = E_{end} = -0.7$ *V*, $E_{inv} = +0.5$ V with $25 \leq v \leq 200$ mV s^{-1} using KCl 0.1 mol L^{-1}, deaerated with N_2, as supporting electrolyte, in the absence and presence of Cu(II) ions. The Cu(II) ions were added in concentrations of $(0.99 \leq C_{Cu(II)}) \leq 6.18) \times 10^{-5}$ mol L^{-1}. The electrochemical cell was a cell of 20 mL with a set of three electrodes: *1*- Pt working electrode with geometric area, $A = 0.0314$ cm^2, modified with SWy-1:8-HQ composite; *2*- reference electrode Ag/AgCl, KNO3(sat.) ($E =$ 465 mV/ERH); and *3*- Ir foil counter electrode ($A = 1.025$ cm^2). Other experimental specific conditions used were added to the text, for clarity.

Spectrophotometry (UV) and molecular fluorescence measurements

Uv–vis spectra of the SWy-1:8-HQ suspensions were obtained in the presence of Cu(II) ions for $(1.01 \leq C_{Cu(II)} \leq 16.0) \times 10^{-6}$ mol L^{-1}. $C_{8\text{-HQ}} = 4.46 \times 10^{-5}$ mol L^{-1} in order to study the formation of possible complex species, Cu(III)-8-HQ, and their effect on the spectra profiles using a UV–Vis Cary 1 E (Varian), with quartz cells 1.00 cm optical path, in the interval from 200 to 300 nm. Molecular fluorescence spectra of the SWy-1:8-HQ suspensions were obtained in the presence of Cu(II) ions for $(1.67 \leq C_{Cu(II)} \leq 29.9) \times 10^{-6}$ mol L^{-1} at $T = (25 \pm 2)$ °C, using a Hitachi recording spectrofluorometer F 4500 type. The excitation was carried out with light of 240 nm using a high-pressure mercury-vapor lamp. The fluorescence spectra were measured by a wavelength ranging from about 300 to 600 nm at 200 nm min^{-1} and excitation/emission slit 5/5 nm.

Thermal Characterization and X-ray diffraction of composites

The SWy-1 composite samples previously prepared: 8-HQ (item *a*); *b)* in the presence of Cu(II) ions, mass of 7 mg, were subjected to a heating rate of $\beta = 20$ °C min^{-1} in a dynamic air atmosphere, with a flow rate of 50 mL min^{-1} using an alumina crucible to obtain TG-DTA simultaneous curves by the thermoanalyser TA-Instruments SDT2960 model, in the temperature range from 25 to 1200 °C, using a crucible of Al_2O_3. DSC measurements of the intercalates and surface layer adsorbed binary and ternary complexes were performed in a synthetic air atmosphere or a pure nitrogen one with a flow rate of 50 mL min^{-1} at a heating rate of $\beta = 5$ °C min^{-1} and samples of about 7 mg by the. An aluminum crucible with a perforated cover ($\phi = 1$ mm) was used for the obtained DSC curves in a TC15-Mettler system, using a DSC-25 module, a TC-15 control unit, and a Stare software. Also, XRD analyses were carried out using a diffractometer Mini Flex II X-Ray Difractometer Rigaku®, Cu $K\alpha = 1.54184$ Å, $(3 \leq 2\theta \leq 40^{\circ})$, step $= 0.05^{\circ}$, an accelerating voltage of 40 kV, and beam current of 15 mA.

Results and discussion

Thermal and X-ray diffraction (XRD) studies of the $\{[>Si–O]_n[Cu(III)(OH_2)_n:(8\text{-HQ})k]\}^{2-n-k}$ composite

Thermal analysis techniques (Fig. 1, simultaneous DTG-DTA; Fig. 2, DSC) were used to investigate the $\{[>Si–O]_n[Cu(II):(8\text{-HQ})_k]\}^{+2-n-k}$ = [SWy-1:Cu:8-HQ] and $\{[>Si–O]_n[(8\text{-HQ})_k:Cu(II)(OH_2)]\}^{+2-n-k}$ = [SWy-1:8-HQ:$Cu(OH_2)$] ternary composites and [SWy-1:$Cu(II)(OH_2)_n$] = [SWy-1:$Cu(OH_2)_n$] and $\{[>Si–O]_n[(8\text{-HQ})_k]\}^{-n-k}$ = [SWy-1:8-HQ] in an oxidizing air atmosphere of nitrogen when necessary.

XRD data (Table 1) and thermal analysis together with molecular fluorescence spectroscopy (MFS), UV-spectroscopy, and cyclic voltammetry (CV) techniques were used to propose the possible structure of the ternary clay complex. The last three techniques will be discussed later.

The DTG-DTA simultaneous curves (Fig. 1) may indicate the removal of volatile species from the surface of the ternary and binary composite and identify the stages of complex degradation as a function of the TG temperature. X-ray diffractograms (XRD) with DTG, DTA and DSC data and molecular fluorescence spectroscopy evaluated

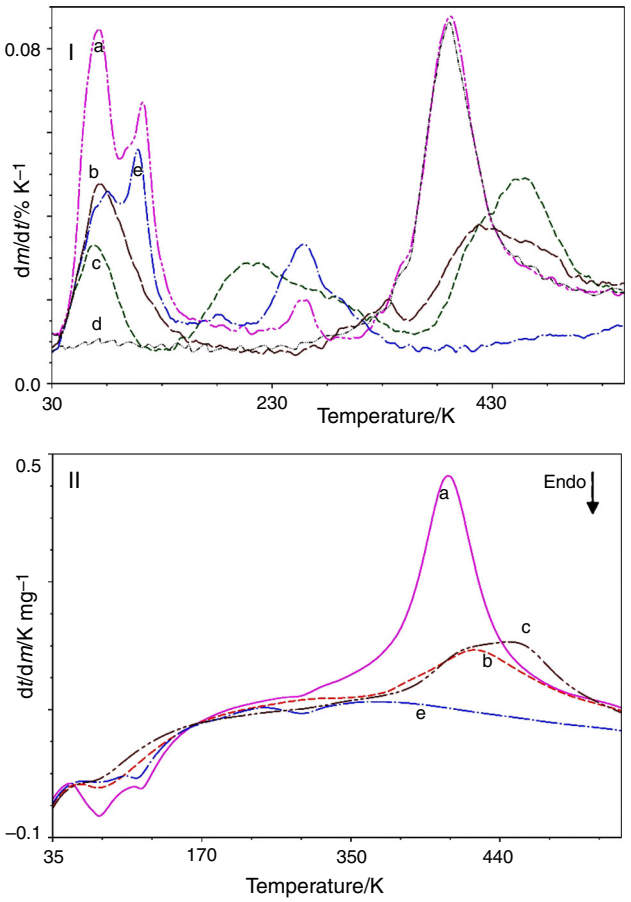

Fig. 1 DTG(I) and DTA(II) curves for the ternary complex: **I***a* and **II***a* [SWy-1:8-HQ:Cu(OH_2)]; **I***d* idem **I***a* heated at $T_{iso} = 285$ °C for 5 min, [SWy-1:8-HQ:Cu]; **I***b* and **II***b* [SWy-1:Cu:8-HQ]; **I***c* and **II***c*) [SWy-1:8-HQ]; **I***e* and **II***e*) [SWy-1:Cu(OH2)n]; sample mass: 7.0 mg; $\beta = 20$ °C min^{-1}; alumina crucible: 70 μL; synthetic air flow = 50 mL min^{-1}

changes in the opening of the interlayer spaces (d_{001}) and its structural surface rearrangement caused by the complex formation between aqueous complex [Cu(II)(OH_2)$_4$] ions and the 8-HQ molecules present in the original binary composites, [SWy-1:8-HQ] [43] and [SWy-1:Cu(OH_2)$_n$].

Figure 1, curves *Ia* – *Ie*, represents the DTG curves obtained in an air oxidizing atmosphere. The *Ia* profile shows the mass loss of ternary complex, [SWy-1:8-HQ:Cu(OH_2)], occurring in four steps, corroborating the DTA and DSC data (Fig. 1.II, 2.I), as follows: (1) the first and second steps were ascribed to the elimination of solvent molecules: 1.1 water molecules adsorbed on clay system surface (1.06% in mass); and 1.2- other water molecules bonded to SWy-1 by a hydrogen-bond inside the interlayer spaces (0.56% in mass); occurring in an endothermic process ($T_{max} = 70$ and 113 °C), in the temperature range between 25 and 175 °C; (2) the third step was ascribed to the endothermic elimination of water molecules ($T_{peak} = 262$ °C) strongly coordinated to Cu(II) ions in the ternary complex (0.19% in mass); and (3) the fourth step was ascribed to oxidation of 8-HQ molecules in the anhydrous ternary complex (2.05% in mass), occurring as an intense exothermic process ($T_{peak} = 392$ °C) from 300 up to 550 °C, anticipating by 58 °C this event in comparison with binary complex, [SWy-1:8-HQ], Fig. 1.I ($T_{peak} = 418$ °C), Fig. 1.II, and Fig. 2.I, curve c; in this event the 8-HQ molecules were eliminated as quinoline-N-oxide (O ← :8-HQ) specie [44].

Figure 1.I *curve b*, corroborated by Figs. 1.II and 2.I *curve b*, shows the profile of the DTG, DTA and DSC curves obtained for ternary complex,[SWy-1:Cu:8HQ]. This complex differently from [SWy-1:8-HQ:Cu(OH_2)] only shows water molecule elimination in the temperature range from 35 to 150 °C, ascribed to solvent elimination from SWy-1 surface.

The mass loss for this complex occurs in three steps: (1) the first one was ascribed to the elimination of solvent molecules adsorbed on the SWy-1 surface layers (2.21% in mass), occurring as an intense endothermic process ($T_{peak} = 73$ °C), in the temperature range from 35 to 145 °C; (2) the second step is indicated by a peak of low intensity and was ascribed to 8-HQ molecules strongly adsorbed in the SWy-1 surface layers (0.25% in mass), occurring in an endothermic process ($T_{peak} = 335$ °C) in a temperature range between 270 and 350 °C; and (3) the third step was ascribed to oxidation of the 8-HQ molecules complexed to Cu(II) ions (3.0% in mass), occurring in a large exothermic process ($T_{peak} = 418$ °C), in the temperature range between 350 and 540 °C; in this event the 8-HQ molecules were eliminated as quinoline-N-oxide (O ← :8-HQ) species [44] and the anticipation of the event a $\Delta T = 33$ °C in comparison to the binary composite [SWy-1:8-HQ] in Fig. 1.1 curve *c* ($T_{peak} = 451$ °C).

Figure 1.I curve *d* shows the DTG response for the previously dehydrated ternary complex [SWy-1:8-HQ:Cu(II)(OH_2)]; the water molecules ($T_{peak} = 262$ °C) were removed by applying an isothermal heating at $T_{isothem} = 285$ °C for 5 min. It is important to note the DTG profile did not show the expected increase in the T_{peak} for trapped 8-HQ molecule removal (4.32% in mass) after dehydration, as observed for the ternary complex of Fe(III) ions [42]. In this way, it can be supposed that the heat released in the oxidation step is enough to eliminate the 8-HQ molecules from the ternary complex present inside and outside the interlayer clay before closing the interlayer space; the heat released causes the anticipation of the event at $\Delta T = 58$ °C in comparison to the binary composite [SWy-1:8HQ].

Figure 1.I, II, curve c, and Fig. 2.I curve c show the profiles of TG, DTA and DSC curves obtained for the binary complex [SWy-1:8-HQ] in air atmosphere, and Fig. 2.II curve c shows the corresponding profiles obtained

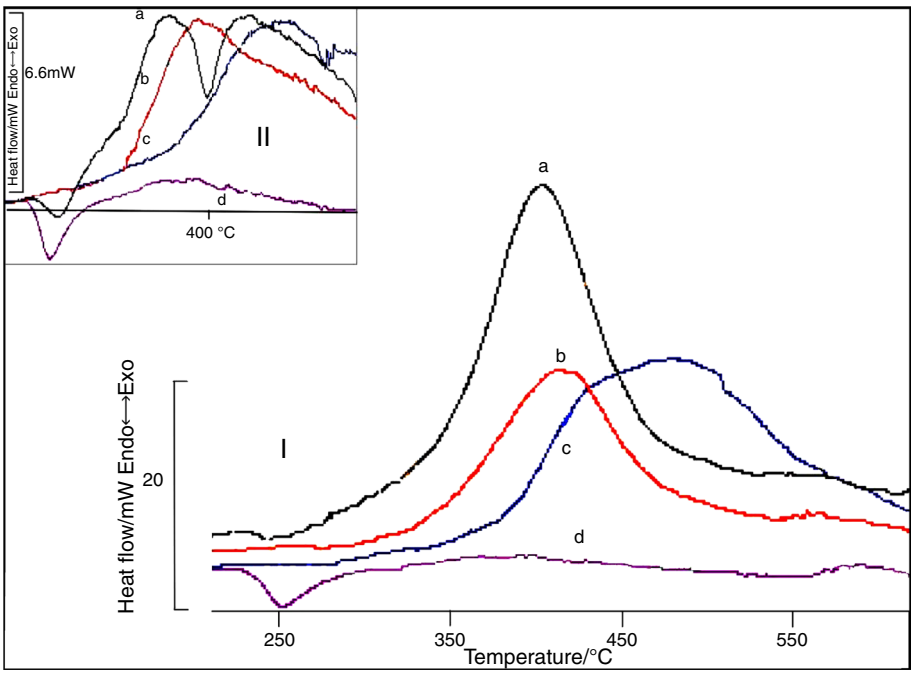

Fig. 2 DSC curves for the ternary and binary complex: **a** [SWy-1:8-HQ:Cu(OH$_2$)], **b** [SWy-1:Cu:8-HQ], **c** [SWy-1:8-HQ] and **d** [SWy-1:Cu(OH$_2$)$_n$]; sample mass: 7.0 mg; $\beta = 20$ °C min^{-1}; alumina crucible: 70 μL; synthetic air **1**) and **2**) N_2, flow = 50 mL min^{-1}

Table 1 d_{001} XRD data obtained for different SWy-1 complexes

Composite	D_{001}/Å	Δd_{001}/Å[a]	Δd_{001}/Å[b]	Remarks
[SWy-1]	12.17	–	–	H_2O $_{interlayer}$
[SWy-1:8-HQ]	14.18	2.01	–	8-HQ $_{interlayer}$
[SWy-1:Cu:8-HQ]	16.99	4.82	2.81	Complex $_{interlayer\ anhydrous}$
[SWy-1:8-HQ:Cu][c]	16.78	4.61	2.60	Complex $_{interlayer\ dehydated}$
[SWy-1:8-HQ:Cu(OH$_2$)]	18.22	6.05	4.04	Complex $_{interlayer\ hydrated}$

[a] $\Delta d_{001} = (d_{001}$ complex - d_{001} [SWy-1])

[b] $\Delta d_{001} = (d_{001}$ complex - d_{001} [SWy-1:8-HQ]). All substances prepared the same way

[c] Complex previously dehydrated: heated at $T_{iso} = 285$ °C/5 min

in a nitrogen atmosphere. These curves are in agreement with each other showing that changes in the atmosphere do not change the profile of the curves. Thus, the thermal decomposition of the binary complex [SWy-1:8-HQ] occurs in three steps as follows: 1- The first step was ascribed to the solvent removal from the clay surface (0.85% in mass), occurring as an intense endothermic process ($T_{peak} = 60$ °C), in the temperature range from 35 to 125 °C; 2- the second step was ascribed to the sublimation removal of 8-HQ molecule dimmers strongly adsorbed on SWy-1 surface (2.16% in mass), occurring as a large endothermic process ($T_{peak} = 208$ °C) in the temperature range from 135 to 382 °C, as pointed out by Pastre et al. [42]; and 3- the third step was ascribed to 8-HQ monomer molecules strongly adsorbed into the SWy-1 (7.55% in mass), occurring as a large endothermic process ($T_{peak} = 451$ °C) in the temperature range from 382 to 550 °C; in this step, the 8-HQ monomer molecules trapped in the interlayer spaces are thermally degraded in CO_2 and water molecules [43].

Figures 1 and 2 curves show the thermal decomposition of the binary complex [SWy-1:Cu(OH$_2$)n]. These curves only show the processes of water removal from the Cu(II) aqueous complex of adsorbed copper ions to the SWy-1. The dehydration process occurs in four steps as follows: 1- the first (3.10% in mass) and second (3.85% in mass) steps are partially overlapped and were ascribed to the solvent removal from SWy-1 surface and from Cu(II) hydrated ions, occurring as an intense endothermic process ($T_{peak} = 83$ and 108 °C), in the temperature range from 35 to 150 °C; 2- the third step was ascribed to water removal from SWy-1 interlayer (0.03% in mass), occurring at a low endothermic process at $T_{peak=}$ 182 °C; 3- fourth step was ascribed to water removal from the hydrated binary complex (1.13% in mass) of [SWy-1:Cu(OH$_2$)$_n$].

From the comparison between curves (Figs. 1, 2), the profiles of the DTG, DTA and DSC curves can be shown by adding hydrated Cu(II) ions into: 1-SWy-1 matrix to form a binary hydrated complex [SWy-1:Cu$(OH_2)_n$]; and 2- binary complex [SWy-1:8-HQ] to form a ternary complex [SWy-1:8-HQ:Cu(OH_2)]; and the addition of 8-HQ to the hydrated binary complex [SWy-1:Cu$(OH_2)_n$] to form a ternary complex [SWy-1:Cu:8-HQ]. These profile changes are in agreement with XRD data, Table 1, and make evident that the experimental method used to prepare the ternary complexes leads to different structural composites. XRD data, Table 1 showed an increase in the interlayer spaces in the transition from pure clay (SWy-1) to the binary and ternary complexes.

These data suggest a possible mechanism to form the ternary complexes: 1- [SWy-1:Cu:8-HQ] – 1.1- at the first step a partial displacement of the water molecules occurs from the hydrated Cu(II) ions resulting in complexation with SWy-1 silanol groups; and 1.2- in the second step the total water molecules displacement from the binary partially hydrated complex occurs [SWy-1:Cu$(OH_2)_n$] by 8-HQ complexation to form a ternary complex, [SWy-1:Cu:8-HQ]; 2- [SWy-1:8-HQ:Cu(OH_2)] – 2.1- at the first step the insertion of 8-HQ molecules into the SWy-1 occurs by molecule adsorption and molecules are present in the interlayer spaces as a packing at a tilted angle, minimizing the solvent content in the SWy-1 surface (solvent content: 0.85% in mass); 2.2- at the second step, hydrated Cu(II) ions are complexed into a binary structure by 8-HQ molecules to form the ternary complex retaining still water molecules previously coordinated to Cu(II) ions.

Calculations made from DTG data allow us to suggest a previous stoichiometry of the ternary complex: [SWy-1:8-HQ:Cu(OH_2)]. The absence and presence of water molecules in these complexes are corroborated by the DSC curves obtained in a different gas atmosphere. Figure 2.I and II, curve a, shows strong evidence for the effective presence of water molecules in the ternary complex [SWy-1:8-HQ:Cu(OH_2)] when a nitrogen atmosphere was used. In this way, the water removal from the complex was favored by the inversion in the thermal event, which has changed from an exothermic to an endothermic reaction; this artifice made the water molecules in the hydrated complex [SWy-1:8-HQ:Cu(OH_2)] evident, and its absence in the complex [SWy-1:Cu:8-HQ].

The thermal experiments conducted by the DSC technique, Fig. 2, under an oxygen or nitrogen atmosphere, especially for [SWy-1:8-HQ:Cu(OH_2)] and [SWy-1:Cu:8-HQ], aim to differentiate the thermal process of 8-HQ removal from the ternary complexes and shows the difference between the two ternary complexes formed by a different experimental way as previously discussed.

Thus, in N_2 atmosphere, the DSC curve (Fig. 2.II, curve *a*) shows an endothermic process with $T_{peak} = 400$ °C, occurring from 365 up to 430 °C, and was ascribed to 8-HQ molecule removal in a distillation process, instead of an exothermic peak ($T_{max} = 392$ °C) as previously observed (Fig. 2.I, curve a); in Fig. 2.II, curve *a,* still remains a rapid kinetic process. On the other hand, by changing the gas atmosphere, the DSC profiles are not changed (Fig. 2.I and II, curve *c*) for the ternary complex [SWy-1:Cu:8-HQ] and the samples show the same temperature peak at $T_{peak} = 405$ °C, evidencing the absence of water molecules in the complex structure from 240 to 350 °C.

This thermal behavior suggests that the Cu(II) ions are inserted in the clay structure, between silanol groups and a dehydrated form. It can be observed that insertion of 8-HQ molecules into the clay structure promotes the complexation of Cu(II) ion, a total water elimination from the interlayer spaces [43] and a consequent contraction of interlayer space (see XRD Table 1). This difference in thermal behavior is caused by the difference in geometry of the ternary complex; in this case, with 8-HQ molecules present in the planar orientation with respect to internal surfaces of the SWy-1 interlayer space.

After discovering the apparent stoichiometry of the ternary complex $\{[>Si–O]n[(8\text{-}HQ)_k{:}Cu(II)(OH_2)]\}^{+2-n-k}$, the apparent geometry was investigated. Thus, XRD data were obtained for the different systems: *a*- pure clay (SWy-1) represented as a silanol group [> Si–O] in the binary and ternary complex formula; *b*- binary complex $\{[>Si–O]_n{:}(8\text{-}HQ)_k]\}^{+2-n-k}$ = [SWy-1:8-HQ]); $(\{[>Si–O]_n{:}Cu(II)(OH_2)]\}^{+2-n-k}$ = [SWy-1:Cu$(OH_2)_n$]; and c- ternary complex $\{[>Si–O]_n[Cu(II){:}(8\text{-}HQ)k]\}^{+2-n-k}$ = [SWy-1:8-HQ:Cu]; $(\{[>Si–O]n[(8\text{-}HQ)k{:}Cu(II)(OH_2)]\}^{+2-n-k}$ = [SWy-1:8-HQ:Cu(OH_2)], all composites were prepared in the same way (Table 1).

Data in Table 1 show that the interlayer space opening increased steadily in the transition from pure clay (SWy-1) to the binary composite, by the intercalation of 8-HQ molecules into SWy-1 and later with the complexation of Cu(II) ions by the 8-HQ molecules. So, the maximum aperture of the interlayer spaces occurs when Cu(II) ions are complexed by 8-HQ molecules present into the binary complex [SWy-1:8-HQ]. This major interlayer opening observed for this ternary compound is of $\Delta d_{001} = 4{,}04$ Å and is not greater than the opening obtained for the binary composite such as prepared in an excess of 8-HQ molecules ($\Delta d_{001} = 4.15$ Å) by Pastre et al. and others [36, 42, 44, 45].

On the other hand, when the ternary complex [SWy-1:Cu:8-HQ] is prepared by the addition of 8-HQ molecules into the binary complex [SWy-1:Cu(OH_2)n] the formed composite shows an interlayer space of, $\Delta d_{001} = 1.67$ Å,

such as that reported by Pastre et al. [43] in the absence of copper ions and the presence of a low quantity of 8-HQ molecules ($\Delta d_{001} = 1.28$ Å) [43]. Figures 1 and 2 and Table 1 indicate different amounts of water molecules in the solid ternary and binary composites, and clay substrate: 1- 3.88% to [SWy-1:8-HQ:Cu(OH$_2$)]; 2- 2.42% to [SWy-1:Cu:8-HQ]; 3- 2.35% to [SWy-1:Cu(OH$_2$)$_n$]; and 4- 1.32% to [SWy-1]. The different water contents are dependent on the experimental preparation conditions and corroborate XRD data in Table 1, showing that the interlayer space opening increased steadily in the transition from pure clay (SWy-1) to the binary or ternary complexes. The increasing in the interlay space is in agreement with the net content of water molecules carried into the clay by the Cu(II) ions complexation when forming the ternary complex [SWy-1:8-HQ:Cu(H$_2$O)], and is in according to the Lewis acid character of the Cu(II) ions as previously discussed.

Figure 3 shows the fluorescence emission spectrum, not normalized, obtained in the UV–visible region ($300 \leq \lambda \leq 550$) nm for the suspensions prepared with the complex [SWy-1:8-HQ] (curve 1: [SWy-1:8-HQ] $\lambda_{excitation} =$ 280 nm and $d_{001} = 14.18$ Å; curve b: [SWy-1:8-HQ:Cu(OH$_2$)], $\lambda_{excitation} = 240$ nm and $d_{001} = 18.22$ Å). The emission fluorescence spectrum obtained for the ternary complex [SWy-1:8-HQ:Cu(OH$_2$)] and binary [SWy-1:8-HQ] shows (curve *a*): 1- a large emission band in the UV–visible range ($350 \leq \lambda \leq 500$) nm, with evidence of peaks in $\lambda = 399$ and $\lambda = 422$ nm; 2- an excimer fluorescence signal in a visible range of ($517 \leq \lambda \leq 567$) nm with peak evidence at $\lambda = 539$ nm; both peaks showing low quantum efficiency. These emissions at $\lambda = 399$ and $\lambda = 422$ nm are of a small intensity, but easily verified when the solid samples are directly illuminated and observed by the naked eye [45–47].

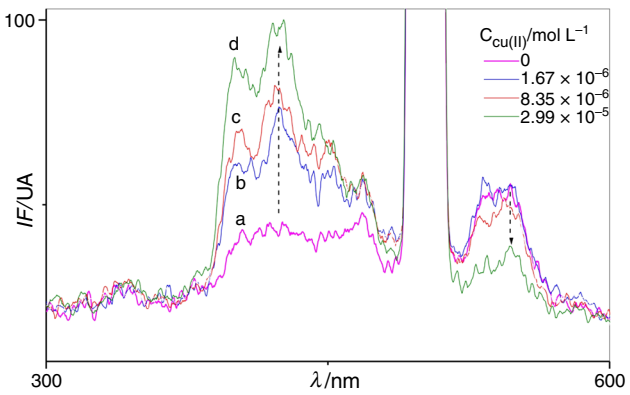

Fig. 3 Fluorescence spectra of ternary complex, [S:8-HQ:Cu(OH$_2$)]: **a** in absence of Cu(II) ions, [SWy-1:8-HQ] binary complex; **b**–**d** increasing Cu(II) ions concentration (inside figure). $C_{8\text{-HQ}} = 4.46 \times 10^{-5}$ mol L^{-1}. pH 6. SWy-1$_{suspension} = 0.11$ gL^{-1}. $\lambda_{excitation} =$ 240 nm. $T = (25 \pm 2)$ °C

The intercalated ternary complex [SWy-1:8-HQ:Cu(OH$_2$)] shows an intensification of a vibrational unfolding spectrum (curve *b* to *e; see arrow inside* Fig. 3) in comparison with curve *a* from the binary complex [SWy-1:8-HQ] when Cu(II) ion concentration is increased in the suspension. On the other hand, it is important to point out the minimization in fluorescence intensity of the excimer at $\lambda = 539$ nm (see arrow inside Fig. 3) when Cu(II) ions were added to the binary complex [SWy-1:8-HQ] suspension. This behavior is in accordance with the dissociation of the excimer present on the surface during the Cu(II)-8HQ complexation.

The observed vibrational unfolding increasing at $\lambda = 399$ and 422 nm was ascribed to an increase in the molecular coplanarity of 8-HQ molecules after the ternary complex formation suggesting that the complex Cu-8HQ was in the interlayer space, rigidly bonded to the substrate viable as a monolayer with the aromatic rings of the complex [8-HQ:Cu(II)(H$_2$O)] at a tilted angle with respect to silica layers.

The XRD data and TG and DSC curves obtained for the binary complex [SWy-1:8-HQ] before the addition of Cu(II) ions are in agreement with Pastre et al. [43] observations for a similar system, where 8-HQ molecules are proposed as a tilted monolayer of 8-HQ molecules given an interlayer space of $d_{001} = 16.64$ Å near the value obtained in this work, $d_{001} = 18.22$ Å. This drawing is in accordance with the results obtained from the DTG, DTA and DSC curves (Figs. 1 and 2) and with the X-ray diffraction data (Table 1). On the other hand, the lowest intensity of the vibrational unfolding observed for [SWy-1:8-HQ] complex suggests that the great majority of 8-HQ molecules are outside the interlayer space. However, as observed from the DTG and DSC curves, molecules inside the interlayer spaces are likely present. It can suggest that the difference observed from the DTG and DSC curves for ternary complexes [SWy-1:Cu:8-HQ] and [SWy-1:8-HQ:Cu(OH$_2$)] is due to the fact that insertion of: 1- 8-HQ molecules into the binary complex of [SWy-1:Cu(OH$_2$)$_n$] generates a ternary complex of [SWy-1:Cu:8-HQ(OH$_2$)] with 8-HQ molecules in a planar geometry relative to Cu(II) ions, which results in the closing of the interlayer space; and 2- 8-HQ molecules into SWy-1 generate the binary complex of [SWy-1:8-HQ] with 8-HQ molecules adsorbed into the SWy-1 surface in a tilted geometry that allows a direct complexation of hydrated Cu(II) ions by the 8-HQ molecules added resulting a hydrated ternary complex as will be discussed later (see reaction 3) in electrochemical investigations of the modified Pt with a thin solid film of [SWy-1:8-HQ].

Figure 4 shows the UV spectra obtained for binary and ternary aqueous suspensions prepared in the same experimental way as samples used for obtaining TG, DTA and

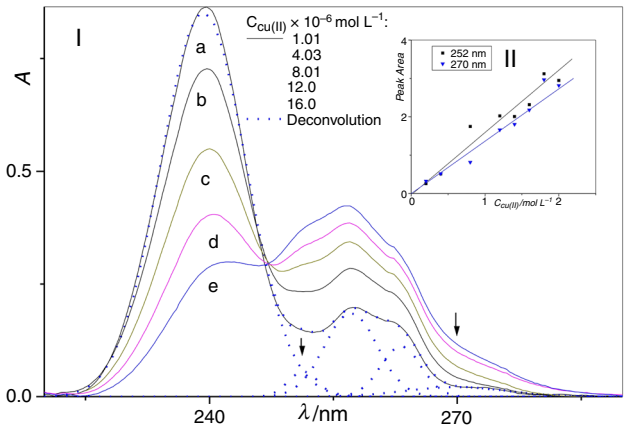

Fig. 4 **I**- curves *a–e* [SWy-1:8-HQ:Cu(OH_2)] system: absorption spectrum obtained from increasing additions of Cu(II) ions ($1.01 \leq C_{Cu(II)} \leq 16.0$) $\times 10^{-6}$ mol L^{-1}. $C_{8\text{-HQ}} = 4.46 \times 10^{-5}$ mol L^{-1}. $T = (25 \pm 2)$ °C; **II**- Lambert–Beer curves at $\lambda = 252$ and $\lambda = 270$ nm; (—) deconvolution of curve *a*

DSC curves and XRD patterns. The complexes were freshly suspended in pure water before using. This figure was obtained from spectrophotometric assays employing an aqueous suspension of the binary composite [SWy-1:8-HQ]: Fig. 4.I- in the presence of Cu(II) ions and Fig. 5II-in the absence of Cu(II) ions. Figure 4.I curves a-i show the UV spectra obtained by the addition of different concentrations of Cu(II) ions ($1.01 \leq C_{Cu(II)} \leq 16.0$) $\times 10^{-6}$ mol L^{-1} to an aqueous binary composite suspension. Figure 4.II shows the Lambert–Beer law obtained for the ternary complex formed [SWy-1:8-HQ:Cu(OH_2)].

These UV spectra show a peak, at $\lambda = 239$ nm ascribed to a hydrophobic dimeric species, $(8\text{-HQ})_2$, on the SWy-1 surface as observed from a florescence study. This species diminished its intensity when Cu(II) ions were added to the suspension at same time that a peak at $\lambda = 252$ nm appeared and intensified; this absorption signal was ascribed to a binary complex formation. Complex formation between [SWy-1:8-HQ] adsorbed molecules [38, 42, 45–48] and Cu(II) ions occurs in accordance with the reaction:

$$*SWy-1:(8-HQ)_2 = 2([SWy-1:8-HQ]) * +2Cu(II) = 2([SWy-1:8-HQ:Cu(OH_2)]);\ (*k = 1.0 \times 10^7\,[43]) \quad (1)$$

According Fig. 4.I the increase in Cu(II) ions concentration causes the appearance of new absorption peaks in the UV range of ($250 \leq \lambda \leq 280$) nm with peaks on $\lambda = 258$ and 272 nm, suggesting the formation of a new species in accordance with the TG, DTA and DSC, fluorescence and XRD data: a ternary complex of [SWy-1:8-HQ:Cu(OH_2)] [49].

Electrochemistry investigation of {Pt/[SWy-1:8-HQ]} binary thin solid film

Cyclic voltammetry technique was used for the electrochemistry study of the Pt-thin solid film electrode of the binary complex [SWy-1:8-HQ] in the absence and presence of Cu(II) ions in water solutions. As a first step we need investigate the mechanical stability of the thin solid film mechanically deposited on the Pt disk surface electrode (geometric area, $A_g = 0.0314$ cm^2). Figure 5.I shows the cyclic voltammograms, CV, obtained from repetitive cyclic voltammetry, for $n = 80$ scan cycles, at 50 mV s^{-1}, in a solution of the supporting electrolyte (KCl, 0.1 mol L^{-1}). These CV profiles show a high mechanical stability for the thin solid film, the absence of an anodic and cathodic peak current in the entire potential range swept and a low capacitive current for the cyclic voltammograms.

The low capacitive current behavior suggests that 8-HQ species are strongly adsorbed onto the clay surface, according to the UV spectra obtained for the same binary composite in a water suspension system (Fig. 4) corroborating the molecular florescence (Fig. 3).

Cyclic voltammetry on {Pt/[SWy-1:8-HQ:Cu(OH_2)]} film modified electrode

The CV profiles of Fig. 5.II were obtained for a fixed concentration of copper ions of 5.58×10^{-5} mol L^{-1} and changing the sweep rate ($25 \leq v \leq 200$) mV s^{-1} to study the electrochemical process occurring on the Pt modified surface. The profiles show a pair of peaks, peaks A and D, mutually interrelated as demonstrated in Fig. 5.III when E_λ, the inversion potential of $\Delta E_\lambda = 0.05$ V, progresses to peak A. The peak potentials are present at 0.14 V (E_A) and at 0.26 V (E_D), respectively, separated by an $\Delta E_p = (68.0 \pm 0.6)$ mV and showing a value of $n = 1.1 \pm 01$ (Table 2); n value was obtained from the relation $\Delta E = 59.1/n$ [50]. This result suggests an electrochemical reversible process; otherwise the profiles pointed out in Fig. 5.IV together with the log i_p versus log v graphic (Fig. 6) suggest, respectively, an electrochemical process controlled by adsorption of the metal ions on the electrode surface. Another important aspect evident in Fig. 5.II is the isopotential point [51] observed at a zero current axis ($I = 0$ A; $E = 0.38$ V); this point denotes the coexistence of two electro active species, but not necessarily in equilibrium and it can be ascribed to the redox pair:

$$Cu(II) + 1e = Cu(I) \quad (2)$$

Figure 5.IV shows the cyclic voltammograms for the modified electrode varying the Cu(II) ions concentration ($0.99 \leq C_{Cu(II)} \leq 5.58$) $\times 10^{-5}$ mol L^{-1} in 0.1 mol L^{-1} KCl. The peak current intensities observed for both peaks

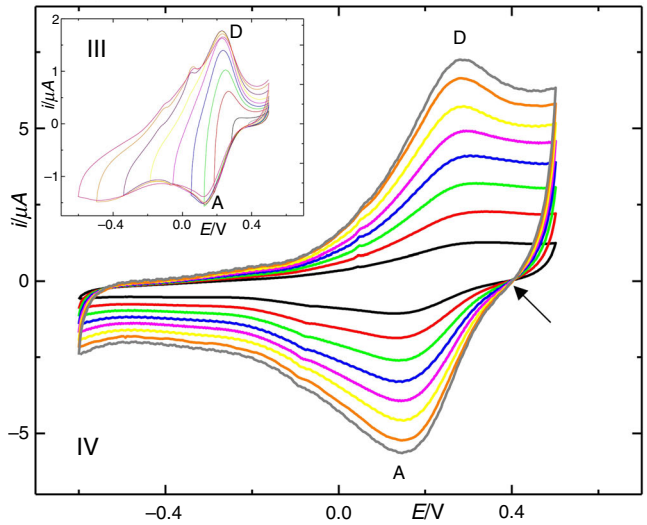

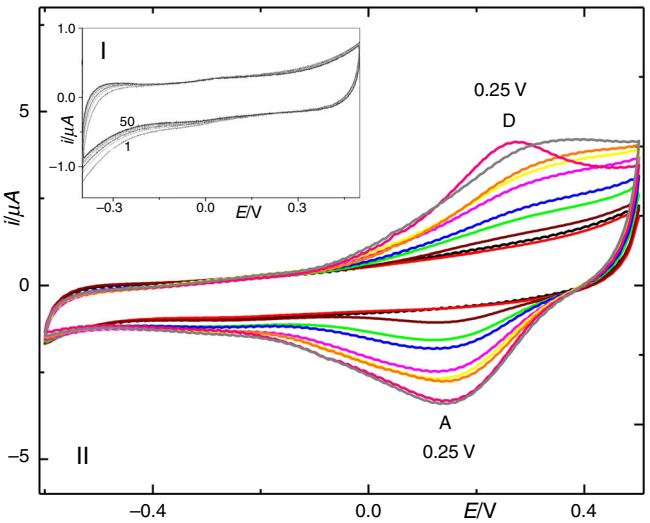

Fig. 5 Cyclic Voltammograms on {Pt/[SWy-1:8-HQ]} modified electrode: **I** to verify mechanical stability $n = 80$ cycles, in absence of Cu(II) ions, $E_{start} = E_{end} = -0.5$ V, $E_{inv} = 0.5$ V. **II**-fixed $C_{Cu(II)} = 9.74 \times 10^{-6}$ mol L^{-1} for sweep rate of $(25 \leq v \leq 200)$ mV s^{-1} ([SWy-1:8-HQ:Cu(OH_2)]). **III**- for E_λ advance on peak A, $C_{Cu(II)} = 5.58 \times 10^{-5}$ mol L^{-1}, $E_i = 0.4$ V, $\Delta E_\lambda = 0.05$ V until $E = -0.4$ V. **IV**- $(0.99 \leq C_{Cu(II)} \leq 6.18) \times 10^{-5}$ mol L^{-1}. For **II** and **IV**: $E_i = E_f = 0.45$ V, $E_{inv.} = -0.6$ V. v = 50 m V s^{-1} except for **II**. KCl 0.1 mol $^{-1}$. $A_g = 0.0314$ cm^2. $T = (25 \pm 2)$ °C. **II-IV**: {Pt/[S:8-HQ:Cu(OH_2)]}

Table 2 Values of E_p^c, E_p^a, ΔE_p e n for different v values, $C_{Cu(II)} = 5.58 \times 10^{-5}$ mol L^{-1}

V/mV s^{-1}	E_p^a/V	E_p^c/V	ΔE_p*	N**
5	0.245	0.184	0.061	1.0
50	0.232	0.174	0.058	1.0
75	0.238	0.170	0.068	1.1
100	0.245	0.173	0.072	1.2
125	0.249	0.176	0.073	1.2
150	0.245	0.179	0.066	1.1
175	0.255	0.178	0.077	1.3
200	0.251	0.179	0.072	12

E_p values were obtained from deconvoluted cyclic voltammograms (CV from Fig. 5.II)

* Medium values: $\Delta E_p = (0.068 \pm 0.006)$ V; ** $n = 1.1 \pm 0.1$

A and D increased as a function of the Cu(II) concentration. However, the peak D in the anodic branch of the voltammogram is more intense than the cathodic peak (peak A), suggesting a week adsorption of the product (in this case Cu(II) ions). This electrochemical behavior was maintained and enhanced with increasing Cu(II) ions concentrations: $(6.78 \leq C_{Cu(II)} \leq 16.0) \times 10^{-5}$ mol L^{-1}. The electrochemical results are in agreement with that shown by the molecular fluorescence (Fig. 3), UV spectra (Fig. 4), DTG, DSC curves (Figs. 1, 2), and XRD data (Table 1). Data from Table 1 shows that the clay interlayer space was increased by 2.02 Å in comparison to pure SWy-1 by adding 8-HQ molecules to form [SWy-1:8-HQ] binary complex [43]. Likewise the insertion of Cu(II) ions into binary complex, [SWy-1:8-HQ] ($\Delta d = 2.01$ Å), increased

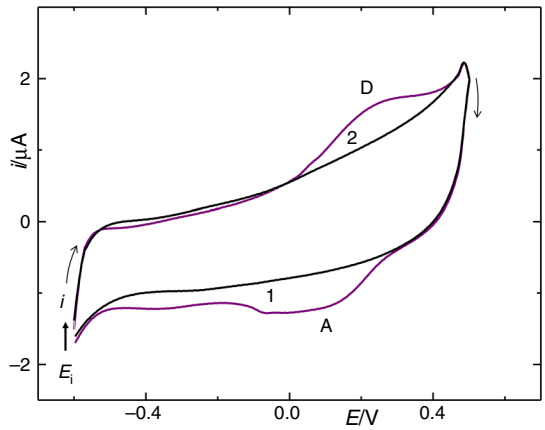

Fig. 6 Cyclic voltammograms obtained on modified thin solid electrodes: 1- in a supporting electrolyte; and 2- after changing the matrix of Cu(II) ions ($C_{Cu(II)} = 6.18 \times 10^{-5}$ mol L^{-1}) by the supporting electrolyte in a washed cell (cell was washed 4 times with a supporting electrolyte before measuring)

the interlayer space from 2.01 to 2.60 Å as the ternary complex is formed [SWy-1:8-HQ]-Cu(II) (Table 1, column 4). The interlayer space enlargement observed in the ternary complex generated an expanded new composite surface film that facilitates the exchange of Cu(II) ions between the solution and film, and vice versa.

Considering the relevant information came from molecular fluorescence, UV–visible spectra and the other techniques used to characterize the film surface before and after the insertion of Cu(II) ions into the binary composite, the electrochemical behavior of peaks A/D from CVs of Fig. 5 were analyzed by applying diagnostic tests for CE

and EC mechanism in agreement with the Greef et al. [52] method. The proposed mechanism for these reaction steps is shown further on in this text.

Homogeneous reactions studies of {Pt/[SWy-1:8-HQ:Cu(OH$_2$)]} thin solid film electrode

Considering the experimental results shown in Fig. 5 and in order to characterize the origin of the coupled redox peaks, A/D, confirm the electrochemical dependence between the coupled peaks and elucidate the mechanisms of electrochemical reactions. Cyclic voltammetric experiments were performed at different v values (Fig. 5.II). Experiments with the inversion of the scanning potential (E_λ) at the peak A (Fig. 5III) were used for $C_{Cu(II)} = 5.58 \times 10^{-5}$ mol L^{-1} and $v = 50$ mV s^{-1} for both potential range of ($-0.60 \leq E_\lambda \leq +0.45$) V for peak A.

Profile analysis of *log* i_p^a versus *log* v graphics, applied to the coupled peaks, A/D (Fig. 1 S in supplementary information), reinforces the adsorption controlled processes occurring at peaks A and D, as in (Fig. 5IV), which corroborated the data obtained by molecular fluorescence and UV-spectra. Another noticeable aspect was the independence of the anodic peak potential E_p^a (peak D) and cathodic peak E_p^c (peak A) with respect to v values (Fig. 1S. in supplementary information).

To elucidate the electrochemical mechanisms which have developed in the coupled peaks, A/D, the current function relationships were used: current function = ($i_p^c/v^{1/2}$) versus v and the ratio of peak currents = i_p^a/i_p^c versus v. Such relationships were obtained for the pair of peaks *A* and *D* separately, and are represented in Fig. 7.I and 7.III for low and high Cu(II) concentrations and in Fig. 7.II for low concentrations, respectively. The evaluation of these curves suggests the presence of a *CE* type mechanism [52] on the ternary complex thin solid film, which displays a rapid chemical kinetic reaction followed by a reversible one-electron transfer process [52]. Thus, considering in a general way, only the aqueous complex species of $[Cu(OH_2)_4]^{2+}$ ~99.9%, present in an aqueous solution at pH 6 [48], a possible mechanism will be suggested as follows: *1* - Chemistry step: a chemical formation of a ternary complex with fast chemical and a reversible one-electron charge transfer reaction on the surface of binary complex;

$$\left\{Pt/[>Si{-}O]_n\left[(8-HQ)_k\right]\right\}^{n-k} + \left[Cu(OH_2)^4\right]^{+2} \gg \left\{Pt/[>Si{-}O]_n[Cu(II)(OH_2) - (8-HQ)k]\right\}^{+2-n-k} + 3H_2O \quad (3)$$

for which n = number of silanol groups; m = number of water molecules*; x = number of water molecules displaced from Cu(II) water complex; k = number of molecules of 8-HQ* [53].

**The number of water (m) and 8-HQ (k) molecules was estimated by DTG primary technique: m = 1 and k = 1.*

The effective confirmation of Cu(II) ion specie retained inside the ternary complex was obtained from the profiles of Fig. 6, obtained for the modified electrode before (only in a support electrolyte) and after use, the electrode in a

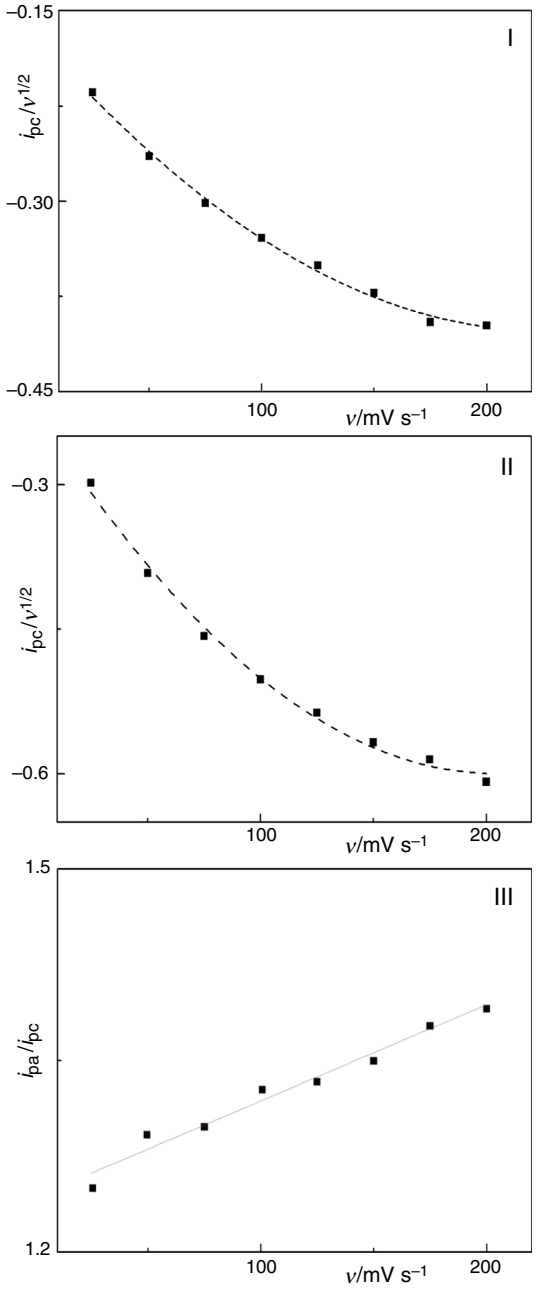

Fig. 7 **I** Current function obtained for the modified thin solid film Pt/[SWy-1:8HQ:Cu(OH$_2$)]} electrode: $\mathbf{i_p^c/v^{1/2}}$ versus $\boldsymbol{v}$ to low $C_{Cu(II)}$; **II**-$\mathbf{i_p^c/v^{1/2}}$ versus $\boldsymbol{v}$ to high $C_{Cu(II)} = 1.99 \times 10^{-4}$ mol L^{-1}. **III**- rate of $\mathbf{i_p^c/i_p^a}$ versus $\boldsymbol{v}$ to low $C_{Cu(II)}$. The range of v *values:* ($25 < \boldsymbol{v} < 200$) mV s^{-1}. $T = (24 \pm 2)$ °C. **I** and **III**: $C_{Cu(II)} = 5.58 \times 10^{-5}$

solution containing Cu(II) ions. These profiles show that the Cu(II) ions were not effectively removed from the modified thin solid film electrode after extensively washing the cell with a support electrolyte, in an specific washed cell. *2*- Electrochemical step: occurring as a rapid and reversible kinetics, transferring only one electron ($n = 1$) from Pt electrode to the Cu(II) ion specie into the ternary complex and reducing it, inside the complex, into a Cu(I) species, generating a new ternary specie of Cu(I) species:

$$\left\{Pt/[>Si{-}O]_n\left[Cu(II)(OH_2)_m{:}\ (8-HQ)_k\right]\right\}^{+2-n-k} + 1e^- = \left\{Pt/[>Si{-}O]_n\left[Cu(I)(OH_2)_m{:}\ (8-HQ)_k\right]\right\}^{+1-n-k}, \quad (4)$$

for which $m = 1$, number of H_2O molecules and $k = 1$, 8-HQ molecule [53]. It is important to point out that SWy-1 clay has charged negative sites, inside and outside the interlayer, that attaches itself to a conductive electron surface [54]. This suggested mechanism is corroborated by information from molecular fluorescence and UV spectra in addition to XRD data and TG, DTA and DSC that provided basis to support the above proposition.

Conclusions

The results of the thermal study (DTG, DTA and DSC) and confirmed by UV–visible, molecular fluorescence spectrophotometry, and XRD, allowed us to propose the structure of the ternary complex composite in agreement with literature [53]: $\{Pt/[>Si{-}O]_n\ [Cu(II)(OH_2)(8\text{-}HQ)]\}^{+2-n}$. The ternary complex has a rigid linear structure, enlarging the interlayer space of the SWy-1 from 2.02 Å to 4.04 Å.

Two peaks with adsorptive characteristics were observed when Cu(II) ions were added to the solution with a weak adsorption of Cu(II) ions.

The A/D pair of peaks were associated to the reversible one-electron transfer involving reduction of Cu(II) species and oxidation of Cu(I) species, with a previous fast coupled chemical reaction, according to a CE mechanism.

The Pt-[SWy-1:8-HQ] thin solid film modified electrode depicted good sensitivity to low concentrations of Cu(II) ions showing that this system has great analytical potentialities.

Acknowledgements The authors thank *CAPES* for the scholarship, FAPERP and *Espaço Magistral, Laboratório de Análises*, Serviços de Apoio Empresarial LTDA for the sponsorship of this work, X CBRATEC/IV CPANATEC, and the Laboratório de Análise Térmica, of the Departament of Analytical Chemistry, São Paulo State University (Unesp), Institute of Chemistry, Araraquara for the thermal studies. The authors and this Foundation have no conflict of interest, regarding this manuscript.

References

1. Gök Ö, Özcan A, Erdem B, Özcan AS. Prediction of the kinetics, equilibrium and thermodynamic parameters of adsorption of copper(II) ions onto 8-hydroxy quinoline immobilized bentonita. Colloid Surface. 2008;317:174–85.
2. Alia RM, Hamada HA, Husseinb MM, Malashb GF. Potential of using green adsorbent of heavy metal removal from aqueous solutions: adsorption kinetics, isotherm, thermodynamic, mechanism and economic analysis. Ecol Eng. 2016;91:317–32.
3. Tokalioglu S, Gurbuz F. Selective determination of copper and iron in various food samples by the solid phase extraction. Food Chem. 2010;123(1):183–7.
4. Aksu ZZ, Isoglu IA. Removal of copper(II) ions from aqueous solution by biosorption onto agricultural waste sugar beet pulp. Process Biochem. 2005;40:3031–44.
5. Wang L, Li J, Jiang Q, Zhao L. Water-soluble Fe3O4 nanoparticles with high solubility for removal of heavymetal ions from waste water. Dalton Trans. 2012;41:4544–51.
6. Zeeb M, Ganjali MR, Norouzi P, Kalaei MR. Separation and preconcentration system based on microextraction with ionic liquid for determination of copper in water and food samples by stopped-flow injection spectrofluorimetry. Food Chem Toxicol. 2011;49:1086–91.
7. Akhond M, Absalan G, Pourshamsi T, Ramezani AM. Gas-assisted dispersive liquid-phase microextraction using ionic liquid as extracting solvent for spectrophotometric speciation of copper. Talanta. 2016;154:461–6.
8. Do Carmo SN, Damásio FQ, Alves VN, Marques TL, Coelho NMM. Direct determination of copper in gasoline by flame atomic absorption spectrometry after sorption and preconcentration on Moringaoleifera husks. Microchem J. 2013;110:320–5.
9. Roldan PS, Alcântara IL, Padilha CCF, Padilha PM. Determination of copper, iron, nickel and zinc in gasoline by FAAS after sorption and preconcentration on silica modified with 2-aminotiazole groups. Fuel. 2005;84(2–3):305–9.
10. Wysocka I, Vassileva E. Determination of cadmium, copper, mercury, lead and zinc mass fractions in marine sediment by isotope dilution inductively coupled plasma mass spectrometry applied as a reference method. Microchem J. 2016;128:198–207.
11. Ceko MJ, Aitken JB, Harris HH. Speciation of copper in a range of food types by X-ray absorption spectroscopy. Food Chem. 2014;164:50–4.
12. Khalil MMH, Shahat A, Radwan A, El-Shahat MF. Colorimetric determination of Cu(II) ions in biological samples using metal-organic framework as scaffold. Sensor Actuat B-Chem. 2016;233:272–80.
13. Ferreira SLC, Queiroz AS, Fernandes MS, dos Santos HC. Application of factorial designs and Doehlert matrix in optimization of experimental variables associated with the preconcentration and determination of vanadium and cop-per in seawater by inductively coupled plasma optical emission spectrometry. Spectrochim Acta B. 2002;57:1939–50.
14. Yu JC, Lo JM, Wai KM. Extraction of gold and mercury from sea water with bismuth diethyldithiocarbamate prior to neutron activation-γ-spectrometry. Anal Chim Acta. 1983;154:307–12.
15. Burrini C, Cagnini A. Determination of mercury in urine by ET-AAS using complexation with dithizone and extraction with cyclohexane. Talanta. 1997;44:1219–23.
16. Ali A, Shen H, Yin X. Simultaneous determination of trace amounts of nickel, copper and mercury by liquid chromatography coupled with flow injection online derivatization and preconcentration. Anal Chim Acta. 1998;369:215–23.
17. Mohadesi A, Taher MA. Voltammetric determination of Cu(II) in natural waters and human hair at a meso-2 3-dimercaptosuccinic acid self-assembled gold electrode. Talanta. 2007;72:95–100.

18. Al-Hossainy AF. Simultaneous determination of Cd(II) and Cu(II) using stripping voltammetry in groundwater, soil and Alhagi maurorum plants in industrial and urban areas in Northern Border, Saudi Arabia with luminol as a chelating agent. Water Sci Technol. 2015;72(7):1127–39.
19. Pereira FJ, Vázquez MD, Debán L, Aller AJ. Inorganic arsenic speciation by differential pulse anodic stripping voltammetry using thoria nanoparticles-carbon paste electrodes. Talanta. 2016;152:211–8.
20. Lin H, Li M, Mihailovič D. simultaneous determination of copper, lead, and cadmium ions at a Mo6S9-xIx nanowires modified glassy carbon electrode using differential pulse anodic stripping voltammetry. Electrochim Acta. 2015;154:184–9.
21. Ghandour MA, Hassan A, Ali HM. Voltammetric determination of copper with proton pump inhibitor drug omeprazole. J Anal Chem. 2015;70(3):392–7.
22. Tonelli D, Scavetta E, Giorgetti M. Layered-double-hydroxide-modified electrodes: eletroanalytical applications. Anal Bioanal Chem. 2013;. doi:10.1007/s00216-012-6586-2.
23. Deng P, Fei J, Zhang J, Li J. Determination of trace copper by adsorptive voltammetry using a multiwalled carbon nanotube modified carbon paste electrode. Electroanal. 2008;20(11):1215–9.
24. Morton J, Havens N, Mugweru A, Wanekaya AK. Detection of trace heavy metal ions using carbon nanotubemodified electrodes. Electroanal. 2009;21(14):1597–603.
25. Mohadesi A, Motallebi Z, Salmanipour A. Multiwalled carbon nanotube modified with 1-(2-pyridylazo)-2-naphthol for stripping voltammetric determination of Pb(II). Analyst. 2010;135(7):1686–90.
26. Ly SY. Diagnosis of copper ions in vascular tracts using a fluorine-doped carbon nanotube sensor. Talanta. 2008;74(5):1635–41.
27. Loudiki A, Boumya W, Hammani H, Nasrellah H, El Bouabi Y, Zeroual M, Farahi A, Lahrich S, Hnini K, Achak M, Bakasse M, El Mhammedi MA. Ibuprofen analysis in blood samples by palladium particles impregnated sodium montmorillonite electrodes: validation using high performance liquid chromatography. Mat Sci Eng C. 2016;69:616–24.
28. Pieganga GBN, Tonle IK, Walcariusc A, Ngamenia E. An inorganic-organic hybrid material from the cointercalation of a cationic surfactant and thiourea within montmorillonite layers: application to the sensitive stripping voltammetric detection of Pb^{2+} and Cd^{2+} ions. Cr Chim. 2016;19(7):789–97.
29. Navrátilová Z, Mucha M. Organo-montmorillonites as carbon paste electrode modifiers. J Solid State Electrochem. 2015;9(7):2013–22.
30. Gholivand MB, Shamsipur M, Dehdashtian S, Adeh NB. Construction of a sensitive sensor for Dpenicillamine using sodium montmorillonite nonoclay as a modifier. J Electroanal Chem. 2014;725:7–11.
31. Beltagi AM, Ghoneim EM, Ghoneim MM. Simultaneous determination of cadmium (II), lead (II), copper (II) and mercury (II) by square-wave anodic stripping voltammetry at a montmorillonite-calcium modified carbon paste electrode. Int J Environ An Ch. 2011;91(1):17–32.
32. Dias Filho NL, Do Carmo DR, Rosa AH. Selective sorption of mercury(II) from aqueous solution with an organically modified clay and its electroanalytical application. Separ Sci Technol. 2006;41(4):733–46.
33. Kula P, Navrátilová Z, Kulová P, Kotoucek M. Sorption and determination of Hg(II) on clay modified carbon paste electrodes. Anal Chim Acta. 1999;385(1–3):91–101.
34. Sun Y, Du H, Deng Y, Lan Y, Feng C. Preparation of polyacrylamide via surface-initiated electrochemicalmediated atom transfer radical polymerization (SI-eATRP) for Pb^{2+}sensing. J Solid State Electrochem. 2015;. doi:10.1007/s10008-015-3008-3.
35. Maghear A, Tertis M, Fritea L, Marian IO, Indreac E, Walcarius A, Săndulescu R. Tetrabutylammoniummodified clay film electrodes: characterization and application to the detection of metal ions. Talanta. 2014;125:36–44.
36. Filho NLD, do Carmo DR. Study of an organically modified clay: selective adsorption of heavy metal ions and voltammetric determination of mercury(II). Talanta. 2006;68:919–27.
37. Navratilova Z, Mucha M. Organo-montmorillonites as carbon paste electrode modifiers. J Solid State Electrochem. 2015;19:2013–22.
38. Khaorapapong N, Ogawa M. Solid-state intercalation of 8-Hydroxyquinoline into Li(I)-, Zn(II)- and Mn(II)-montmorillonites. App Clay Sci. 2007;35:31–8.
39. Keidar O, Lapides I, Shoval S, Yariv S. Thermogravimetry and differential thermal analysis of montmorillonite treated with 1,4-diaminoanthraquinone. J Ther Anal Calorim. 2015;120(1):33–43.
40. Souza MA, Larocca NM, Pessan LA. Highly thermal stable organoclays of ionic liquids and silane organic modifiers and effect of montmorillonite source. J Ther Anal Calorim. 2016;. doi:10.1007/s10973-016-5501-z.
41. Souza GR, Fertonani FL, Pastre IA. Estudo espectro eletroquímico de sistemas estruturados argila-corante. Eclet Quim. 2003;28:77–83.
42. Franzin BT, Lupi CP, Martins LA, Guizellini FC, Santos CCM, Pastre IA, Fertonani FL. Thermal and electrochemical study of Fe(III) organophilic montmorillonite. J Ther Anal Calorim. 2017;. doi:10.1007/s10973-017-6327-z.
43. Pastre IA, Nascimento OI, Moitinho ABS, Souza GR, Ionashiro EY, Fertonani FL. Thermal behaviour of intercalated 8-hydroxyquinoline (oxine) in montmorillonite clay. J Ther Anal Calorim. 2004;75:663–9.
44. Juiz SA, Leles MIG, Caires ACF, Boralle N, Ionashiro M. Thermal decomposition of the magnesium zinc, lead and niobium chelates derived from 8-quinolinol. J Ther Anal Calorim. 1997;50:625–32.
45. Pimchana P, Khaorapapong N, Sohmiyab M, Ogawa M. *In itu* complexation of 8-hydroxyquinoline and 4,4′-bipyridine with zinc(II) in the interlayer space of montmorillonite. Appl Clay Sci. 2014;95:310–6.
46. Khaorapapong N, Pimchan P, Ogawa M. Formation of mixed-ligand zinc(II) complex-montmorillonite hybrids by solid–solid reactions. Dalton T. 2011;40:5964–70.
47. Ghedini M, La Deda M, Aiello I, Grisolia A. Synthesis and photophysical characterisation of luminescent zinc complexes with 5-substituted-8-hydroxyquinolines. J Chem Soc Dalton. 2002;. doi:10.1039/B202945F.
48. Bardez E, Devol I, Larrey B, Valeur B. Excited-state processes in 8-hydroxyquinoline: photoinduced tautomerization and solvation effects. J Phys Chem B. 1997;101:7786–93.
49. Baes CF, Mesmer RE. The hydrolysis of Cations. Library of Congress Cataloging in Publication Data, 1976.
50. Kissinger PI, Heineman WR. Laboratory techniques in electroanalytical chemistry. New York: Marcel Dekker Inc; 1984.
51. Untereker DF, Bruckenstein S. The interpretation of isopotential points at rotating ring-disk electrodes. J Electroanal Chem. 1974;57(1):77–87.
52. Greff R, Peat R, Peter LM, Pletcher D, Robinson J. Instrumental methods in electrochemistry. New York: Wiley; 1985.
53. Sigel H. Coordenation chemistry. Oxford: Pergamon Press; 1980. p. 27–45.
54. Schoonheydt RA, Johnston CT. Surface and interface chemistry of clay minerals. In: Bergaya F, Theng BKG, Lagaly G, editors. Handbook of clay science developments in clay science. Amsterdam: Elsevier; 2006. doi:10.1016/S1572-4352(05)01003-2.